

PATTERN OF LENSED CHIRP GRAVITATIONAL WAVE SIGNAL AND ITS IMPLICATION ON THE MASS AND POSITION OF LENS

DONGZE SUN¹, XILONG FAN²
Draft version November 20, 2019

ABSTRACT

We propose a new measurement strategy of the estimation of the lens mass, as well as the actual amplification, of the lens through the modulation pattern of lensed gravitational wave signals alone. This can be done by measuring the frequency and amplitude ratio of peaks and valleys of the modulation pattern of CBC signals, known as “beat”, which is a time domain phenomenon of strong lens effect.

1. INTRODUCTION

The detection of gravitational waves (GWs) by LIGO/Virgo collaborations LIGO/Virgo collaborations (2016) open the new era of the GW astronomy and the multi-messenger astronomy. If gravitational waves pass through a massive body in the process of propagation, they can be gravitationally lensed. P. Schneider, J. Ehlers, and E. E. Falco (1992). The effects of lensed the tensor wave nature of GW (e.g. rotation of the polarization plane of GW Hou et al. (2019a)) is negligible for most lensed systems. Only the amplification effect (e.g. Takahashi & Nakamura (2003)) of the lens is the investigated in most literature.

In the context of 3rd generation interferometric ground detectors - the Einstein Telescope in particular - quite recent series of papers explored the perspectives of observing gravitationally lensed coalescing double compact objects by the ET for the SIS lens model (Piórkowska, Biesiada & Zhu 2013; Biesiada et al. 2014; Ding, Biesiada & Zhu 2015) and more realistic lens model Li et al. (2018), respectively. Rates of lensed GW in adLIGO were reassessed by Ng et al. (2018), Yang et al. (2019).

Under the geometrical optics approximation, the lensing effects for parameters estimation for individual inspiral signal and the population of black hole mergers were addressed in Cao et al. (2014) and Dai et al. (2017) for ground-based detectors, respectively.

Nakamura (1998) has first taken correct account of the diffraction effect in GW lensing and demonstrated that when the lens is much lighter than $\sim 10^2 M_\odot$, the diffraction is so effective that the geometric optics cannot be used anymore. This subject has been advanced in the papers by Takahashi & Nakamura (2003), Takahashi (2016) and K. Liao, M. Biesiada, and X.-L. Fan (2019).

Given the fact of lacking sky localization ability of GW detectors, previous studies of applications of the lensed gravitational waves as an astrophysical tool focus on the multi-messenger approach, namely people need to identify the host galaxy by their EM counterpart to get the information of source redshift and the lens potential. The GW speed Fan et al. (2017); Baker & Trodden (2017); Collett & Bacon (2017), the Hubble constant Liao et al. (2017) cosmic curvature Li et al. (2019) and dark matter substructure Li et al. (2018) have been studied with the information of the time-delay from GW and redshift

and location from EM signals of a strong lens system. The multi-messenger approach could only apply for the bns signal, while the major detection of GW should be BBH.

Recently, with the beat pattern of lensed GW alone, Hou et al. (2019b) used matched filter strategy to determine the lens mass and the actual amplification of the point mass and SIS model under the geometrical optics approximation assuming known template for the lensed GWs.

In this paper we propose a waveform independent method to measure lens parameters and the actual amplification by the “beat” pattern of the strong lensed gravitational wave. This paper is organized as follows: In section 2 we give the formulation of the lensing effect of GW, and introduce the characteristics of patterns in the lensed signals. In section 3 we provide the condition under which patterns can show up, and we discuss the relationship between the characters of patterns and parameters of both source and lens. Then we present a new approach to detect the information of gravitational lens and GW source. In section 4 we choose the CBC waveform and point-mass lens model as an example, to illuminate the characteristics of patterns we have discussed, and to show how our method works. And we give a summary in section 5.

2. LENSING EFFECT OF GW

In a gravitational lens system, we denote the distances between the source and lens, lens and observer, source and observer as D_{LS} , D_L and D_S respectively, 2 dimensional vector $\boldsymbol{\eta}$ denotes the distance of the source from the attachment of lens and observer, and $\boldsymbol{\xi}$ is a position vector on lens plane.

Following Takahashi & Nakamura (2003), for a monochromatic wave with frequency f , the effect of gravitational lens can be described by amplification factor $F(f)$ defined as:

$$F_{+, \times}(f) = \frac{\tilde{h}_{+, \times}^L(f)}{\tilde{h}_{+, \times}(f)}. \quad (1)$$

The frequency and polarization of the signal is not influenced by the lens and only the amplitude is remodulated.

The amplification factor is given by:

$$F(f, y) = \frac{D_S \xi_0^2}{D_L D_{LS}} \frac{f}{i} \int d^2 \mathbf{x} \exp[2\pi i f t_d(\mathbf{x}, \mathbf{y})], \quad (2)$$

¹ Hongyi Honor School, Wuhan University
² School of Physics and Technology, Wuhan University

where $\mathbf{x} = \boldsymbol{\xi}/\xi_0$, $\mathbf{y} = \boldsymbol{\eta}D_L/\xi_0D_S$, and ξ_0 is an arbitrary normalization constant.

For the ground detectors, the detected signal in time domain is then

$$h^L(t) = [A^+ h_+^L(t) + A^\times h_\times^L(t)], \quad (3)$$

where A^+ and A^\times are antenna pattern of the detector, and $h_{+,\times}^L(t)$ is the lensed GW signal in time domain. Hereafter we assume the antenna pattern is a constant.

2.1. The beat pattern

When the wavelength of source signal is much larger than the Schwarzschild radius of the gravitational lens, there is no pattern but the amplification of the signal. While the wavelength is comparable with the Schwarzschild radius of lens, the patterns show up, and exist when wavelength is small enough to enter the realm of geometric optics. Here we derive the exact condition for the patterns to show up for the strong lensed case.

To analyze the pattern on the lensed signal, we compute the envelope of the signal using Hilbert transform:

$$A^L(t) = \left| \frac{1}{\pi} \int \frac{h^L(\tau)}{t - \tau} d\tau \right|, \quad (4)$$

where $h^L(\tau)$ is the lensed GW signal. The position of peaks and valleys of the envelope are related to the lens mass M_L and position y . Note that for a typical lens (such as SIS and point mass model), the amplification factor is a function of the product of lens mass M_L and the GW frequency f : $w = M_L f$, so the lensed GW signal $\tilde{h}^L(f)$ in frequency domain can be written as:

$$\tilde{h}^L(f) = F(w)\tilde{h}(f), \quad (5)$$

So when the frequency changes slowly (e.g. $\dot{f} \ll f^2$), a necessary condition for peaks of the envelope in this case is:

$$\left. \frac{dF(w)}{dw} \right|_{f=f_p} = 0, \quad (6)$$

where f_p is the frequency of peaks of the envelope. So we have $f_p \propto 1/M_L$ in this case. The condition $\dot{f} \ll f^2$ is valid for all lensed CBCs in the wave region $\lambda \sim R_s$, and even valid for part of optical region, so we can obtain the proportional coefficient in geometric optical region.

$$F(f) = \sum_j \mu_j^{1/2} e^{i2\pi f t_{d_j} - i\pi n_j}, \quad (7)$$

meaning that discrete images interfere with each other, where μ_j is the magnification of the j th image, $t_{d_j} = t_d(\mathbf{x}_j, \mathbf{y})$, and $n_j = 0, 1/2, 1$ when \mathbf{x}_j is a minimum, saddle, and maximum point respectively of $t_d(\mathbf{x}, \mathbf{y})$.

Suppose there are only two images, e.g., in the case of point-mass model and SIS model, if t_0 is the time of n th peak $f_p(n)$ and $t_0 + \Delta t$ is the time of $(n+1)$ th peak $f_p(n+1)$, they must satisfy,

$$\int_{t_0}^{t_0 + \Delta t} [f(\tau) - f(\tau - \Delta t_d)] d\tau \propto 1, \quad (8)$$

where Δt_d is the time delay of two lensed signals. Expand

Eq. 8 in Taylor series:

$$\int_{t_0}^{t_0 + \Delta t} \left[\dot{f}(\tau)\Delta t_d + \frac{1}{2}\ddot{f}(\tau)\Delta t_d^2 + \dots \right] d\tau \propto 1. \quad (9)$$

So in geometric region,

$$\dot{f}(\tau)\Delta t_d \gg \frac{1}{2}\ddot{f}(\tau)\Delta t_d^2, \quad (10)$$

Equation (8) can be integrated as

$$[f_p(n+1) - f_p(n)]\Delta t_d \propto 1. \quad (11)$$

So $\Delta f_{peak} \propto 1/t_d \propto 1/M_L$ when $\dot{f}(\tau)\Delta t_d \gg \frac{1}{2}\ddot{f}(\tau)\Delta t_d^2$.

3. MEASURING THE LENS MASS

3.1. The $f_p - n/M_L$ map

According to the geometric approximation and 11, We obtain the relationship between f_p and M_L , n , and y when $\dot{f}(\tau)\Delta t_d \gg \frac{1}{2}\ddot{f}(\tau)\Delta t_d^2$:

$$f_p = \alpha \frac{n}{\Delta t_d}, \quad (12)$$

Note that this equation is also valid to low frequency region as discussed in section 2.1, just replace t_d with its expression obtained in optical region. This equation implicates that the first peak appears when $f_{peak} = \alpha/\Delta t_d$, where $n = 1$, and Δt_d is given in the optical region. If condition (10) is not satisfied, equation (8) is always valid to describe the $f_{peak} - n/M_L$ map in high frequency region.

3.2. The amplitudes ratio of beat and measurement of the lens mass

If we can measure appearing times or corresponding frequencies of more than two adjacent peaks, we can obtain Δt_d from equation (12) when condition (10) is satisfied, or using (8) when the condition is not satisfied. combining the timedelay information, we could measure the M_L and y by measuring the amplitudes ratio r of valleys and peaks.

The unlensed CBC signal $h(t)$ could be written as:

$$h(t) = \frac{a(M_L, t)}{D_L} b(t) e^{i(\Phi(t) + \phi_0)}. \quad (13)$$

In geometric region, also suppose that there are only two images, the amplitude ratio of a valley at $t = t_1$ and its next adjacent peak at $t = t_2$ can be given by:

$$r = \frac{\cos(\pi n_1) \sqrt{|\mu_1|} b(t_1) - \cos(\pi n_2) \sqrt{|\mu_2|} b(t_1 - \Delta t_d)}{\cos(\pi n_1) \sqrt{|\mu_1|} b(t_2) + \cos(\pi n_2) \sqrt{|\mu_2|} b(t_2 - \Delta t_d)}, \quad (14)$$

where n_1 and n_2 is defined in equation (7). This is because the peaks and valleys appear near the extreme of the two images where $(\Phi(t) + \phi_0)$ approximately equals to 0 or π , so the phase term is eliminated.

The form of $b(t)$ and $(\Phi(t) + \phi_0)$ can be determined by measuring the signal of the second image (after the coalescence of the first image), or by measuring the frequency of signal $f(t)$, since $f(t)$ is not influenced by the lens, as discussed in section 2. From the information of $b(t)$, $(\Phi(t) + \phi_0)$ and the measurement of r , we can obtain y from equation (14), since μ is only a function of y .

Then we can get M_L from the expression of Δt_d , since Δt_d is an expression of M_L and y . Besides, we can also obtain the absolute magnification μ , thus we can also measure the distance D_L of the source.

4. THE APPLICATION ON INSPIRALING COMPACT BINARY

To demonstrate our approach, we adopt the point mass lens model and the newtonian approximation inspiral phase signal. For the newtonian approximation inspiral phase signal, the frequency of GW evolves as

$$f(t) = \frac{5}{4} \left(\frac{5GM_c}{c^3} \right)^{-5/8} (t_{coal} - t)^{-3/8}. \quad (15)$$

In this case, condition (10) $\dot{f}(\tau)\Delta t_d \gg \frac{1}{2}\ddot{f}(\tau)\Delta t_d^2$ is equivalent to

$$t_{coal} - t \gg \frac{11}{16}t_d. \quad (16)$$

The amplification factor (2) of the point mass lens model is analytically given by Takahashi & Nakamura (2003):

$$F(w, y) = \exp \left\{ \frac{\pi w}{4} + i \frac{w}{c} \left[\ln \left(\frac{w}{2} \right) - 2\phi_m(y) \right] \right\} \times \Gamma \left(1 - \frac{i}{2}w \right) {}_1F_1 \left(\frac{i}{2}w, 1; \frac{i}{2}wy^2 \right), \quad (17)$$

where $w = 8\pi M_L f$, $\phi_m(y) = (x_m - y)^2/2 - \ln x_m$ where $x_m = (y + \sqrt{y^2 + 4})/2$, and ${}_1F_1$ is the confluent hypergeometric function. In geometric region, the approximation of amplification factor is:

$$F(f) = \sqrt{|\mu^+|} - i\sqrt{|\mu^-|} e^{i2\pi f \Delta t_d}, \quad (18)$$

where

$$\mu^\pm = \frac{1}{2} \pm \frac{y^2 + 2}{2y\sqrt{y^2 + 4}}, \quad (19)$$

and

$$\Delta t_d = 4 \frac{GM_L}{c^3} \left[\frac{y\sqrt{y^2 + 4}}{2} + \ln \left(\frac{\sqrt{y^2 + 4} + y}{\sqrt{y^2 + 4} - y} \right) \right]. \quad (20)$$

Figure 1 shows the ‘‘beat’’ pattern for the 3-3 M_\odot and 30-30 M_\odot binary black holes. The point lens masses are 1000 M_\odot and 2000 M_\odot , and y are settled as 2 and 3, respectively. On the upper x -axis of these figures, we show

$2\pi R_s/\lambda$ of the signal, which is the criterion of wave region and optical region, and the red lines delineate the boundaries for with condition (10) is satisfied. From these results we can see that the patterns show up when the wavelength is comparable with the Schwarzschild radius of lens, and the positions of peaks before the red line is indicated by equation (12).

To get the coefficients α of equation (12) by fitting approach, we change the mass of lens from 100 M_\odot to 2000 M_\odot , and y from 0.8 to 5.0. As an example, we fix y as 5.0, and plot the $f_{peak} - n/M_L$ map discussed in section 3.1 in Figure 2. We define γ as $t_{coal} - t = \gamma \frac{11}{16} t_d$, and it is obvious that the larger the γ , the better the linear relationship discussed in equation (12) is. And this figure also indicates that the proportional coefficients in high frequency region α are also valid in low frequency region, as discussed in section 2.1 and 3.1, which is $\alpha \approx 1.12$ by fitting.

We also test this formula with different sources and different y , e.g., 30 – 30 M_\odot binary black holes, the lens mass also varies from 100 M_\odot to 2000 M_\odot , and y varies from 1.0 to 5.0. We also fit α by plotting $k - n/\Delta t_d$, and we find that α is also approximate to 1.12. The results are showed in Figure 3.

5. SUMMARY AND OUTLOOK

In this paper, we propose a new method to measure the mass, position and the absolute magnification of gravitational lens for the strong lensed system with GW alone. We focus on the ‘‘betat’’ patterns of lensed GW, and we find the relationship between the frequency of the peaks f_p of the envelope, the amplitude ratio of adjacent valleys and peaks r , and the mass M_L , position y of gravitational lens: equations (8), (12), and (14), where equation (8) and (14) is valid for optical region, and equation (12) is valid for both wave and optical region as long as condition (10) is satisfied. Thus by measuring the corresponding frequencies of more than two adjacent peaks, we can obtain Δt_d from equation (12) or (8). Since the unlensed waveform with the normalized amplitude removed can be easily measured, i.e., $b(t)e^{i(\Phi(t)+\phi_0)}$ in waveform (13), we can obtain the position of lens y using equation (14), then we can obtain the mass of lens M_L , the absolute magnification μ , and therefore the distance of GW source D_L .

The point mass lens model and the BH-BH signals are used to demonstrate our method. This system could be detected in future ground based detectors.

REFERENCES

- B. P. Abbott et al., Phys. Rev. Lett., 116, 061102 (2016), arXiv:1602.03837 [gr-qc]; Phys. Rev. Lett., 116, 241103 (2016), arXiv:1606.04855 [gr-qc]; Phys. Rev. Lett., 118, 221101 (2017), arXiv:1706.01812 [gr-qc]; Phys. Rev. Lett. 119, 141101 (2017), arXiv:1709.09660 [gr-qc]; Phys. Rev. Lett. 119, 161101 (2017), arXiv:1710.05832 [gr-qc]; Astrophys. J. 851, L35 (2017), arXiv:1711.05578 [astro-ph.HE]; B. P. Abbott et al. (LIGO Scientific, Virgo), Phys. Rev. X 9, 031040 (2019), arXiv:1811.12907 [astro-ph.HE].
- P. Schneider, J. Ehlers, and E. E. Falco, Gravitational Lenses (Springer, Berlin, Heidelberg, 1992) p. 560.
- Ackermann, M., Albert, A., Atwood, W. B., et al. 2014, ApJ, 793, 64
- Nakamura T. T., ‘‘Gravitational Lensing of Gravitational Waves from Inspiral Binaries by a Point Mass Lens’’, Phys. Rev. Lett., 80, 1138 (1998)
- Takahashi R., Nakamura T., 2003, ApJ, 595, 1039
- Takahashi R., ‘‘Arrival Time Differences between Gravitational Waves and Electromagnetic Signals due to Gravitational Lensing’’ ApJ, 385, 103 (2017)
- Piorkowska A., Biesiada M. & Zhu Z-H. ‘‘Strong gravitational lensing of gravitational waves in Einstein Telescope’’ JCAP10(2013)022
- Biesiada M., Ding X., Piorkowska A. & Zhu Z-H. ‘‘Strong gravitational lensing of gravitational waves from double compact binaries - perspective for the Einstein Telescope’’ JCAP10(2014)080
- Ding X., Biesiada M. & Zhu Z-H., ‘‘Strongly lensed gravitational waves from intrinsically faint double compact binaries - prediction for the Einstein Telescope’’ JCAP12(2015)006

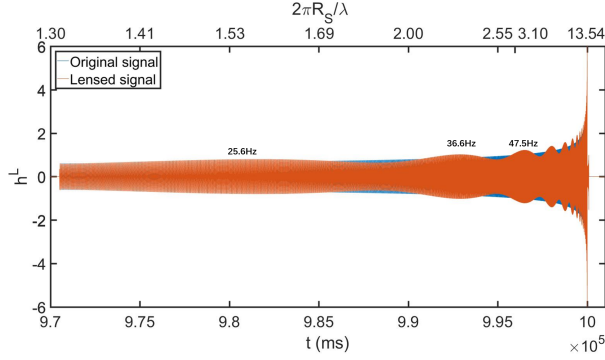
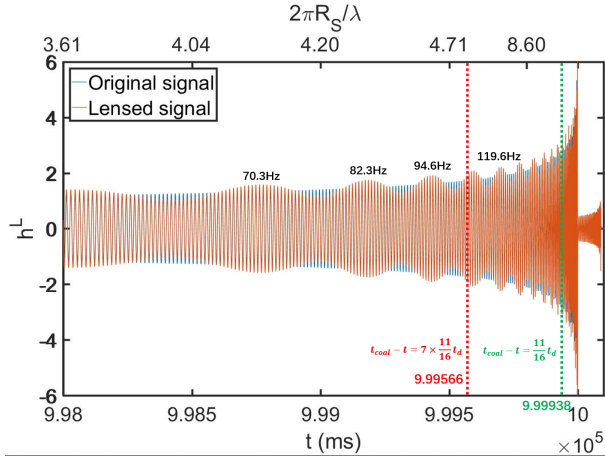
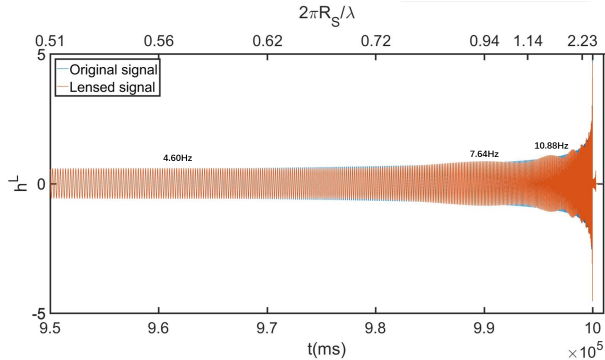
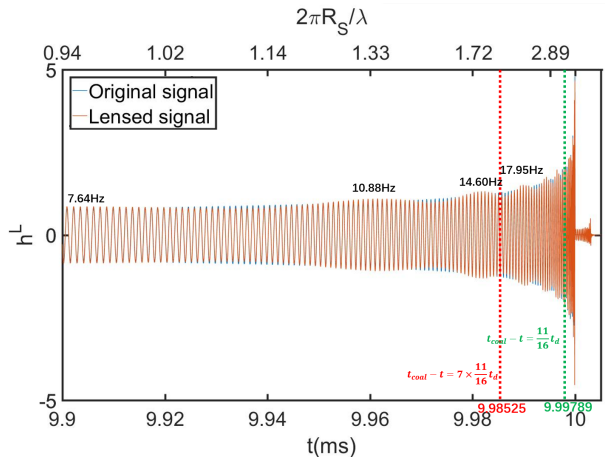
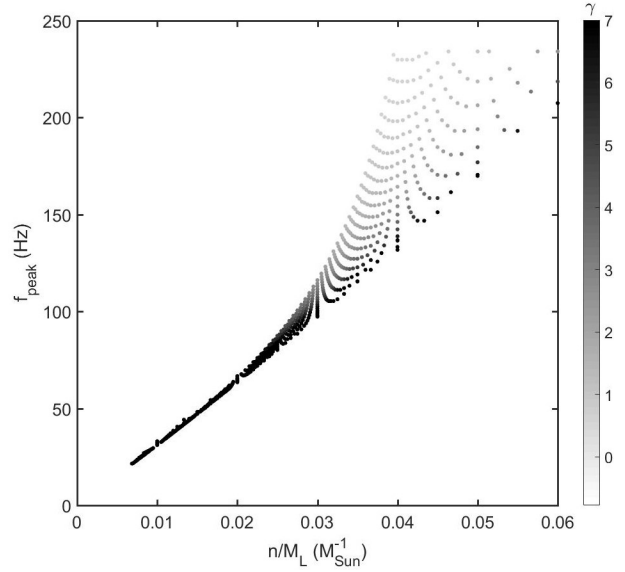
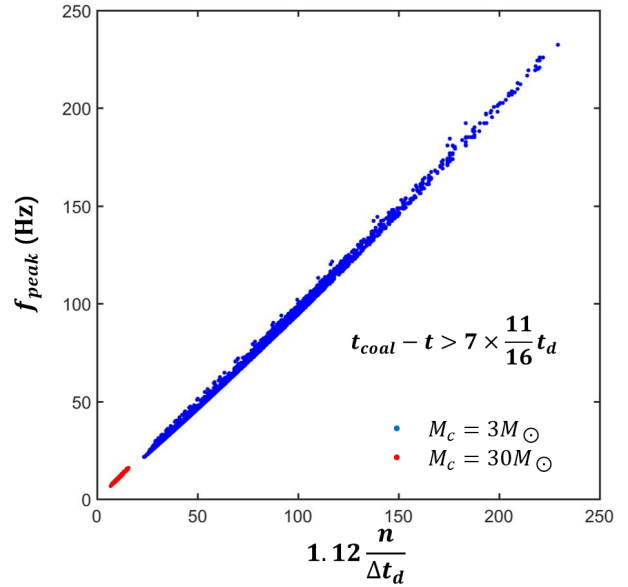
(a) 3-3 M_{\odot} binary black hole, $y = 2.0$, and $M_L = 1000M_{\odot}$.(b) 3-3 M_{\odot} binary black hole, $y = 2.0$, and $M_L = 1000M_{\odot}$.(c) 30-30 M_{\odot} binary black hole, $y = 3.0$, and $M_L = 2000M_{\odot}$.(d) 30-30 M_{\odot} binary black hole, $y = 3.0$, and $M_L = 2000M_{\odot}$.

FIG. 1.— Examples of lensed waveform.

FIG. 2.— The relationship between f_p and n/M_L , $y = 5.0$, M_L varies from $100M_{\odot}$ to $2000M_{\odot}$. Here γ is defined as $t_{\text{coal}} - t = \gamma \frac{11}{16} t_d$.FIG. 3.— The verification of equation (12) using 30–30 M_{\odot} binary black holes. The lens mass also varies from $100M_{\odot}$ to $2000M_{\odot}$, and y varies from 1.0 to 5.0.

- Li S-S., Mao S., Zhao Y., Lu Y., "Gravitational lensing of gravitational waves: A statistical perspective" MNRAS 476, 2220-2229 (2018)
- Ken K. Y. Ng, Kaze W. K. Wong, Tjonnie G. F. Li, & Tom Broadhurst "Precise LIGO Lensing Rate Predictions for Binary Black Holes" Phys. Rev. D 97, 023012 (2018)
- Zhoujian Cao, Li-Fang Li. & Yan Wang "Gravitational lensing effects on parameter estimation in gravitational wave detection with advanced detectors" Phys. Rev. D 90, 062003 (2014)
- Liang Dai., Tejaswi Venumadhav. & Kris Sigurdson "Effect of lensing magnification on the apparent distribution of black hole mergers" Phys. Rev. D 95, 044011 (2017)
- Liao K., Fan X-L., Ding X., Biesiada M. & Zhu Z-H., "Precision cosmology from future lensed gravitational wave and electromagnetic signals" Nature Comm. 8:1148 (2017)
- Hou S., Fan X-L., & Zhu Z-H., S. Hou, X.-L. Fan, K. Liao, and Z.-H. Zhu, arXiv:1911.02798 [gr-qc].

- Fan X.-L., Liao K., Biesiada M., Piórkowska-Kurpas A., Zhu Z.-H., "Speed of gravitational waves from strongly lensed gravitational waves and electromagnetic signals" , Phys. Rev. Lett. 118, 091102 (2017)
- S. Hou, X.-L. Fan, and Z.-H. Zhu, Phys. Rev. D 100, 064028 (2019), arXiv:1907.07486 [gr-qc].
- Baker, T. & Trodden, M., "Multi-Messenger Time Delays from Lensed Gravitational Waves" Phys. Rev. D 95, 063512 (2017)
- Thomas E. Collett & David Bacon., "Testing the Speed of Gravitational Waves over Cosmological Distances with Strong Gravitational Lensing" , Phys. Rev. Lett. 118, 091101 (2017)
- K. Liao, M. Biesiada, and X.-L. Fan, Astrophys. J. 875, 139 (2019), arXiv:1903.06612 [gr-qc].
- Lilan Yang, Xuheng Ding, Marek Biesiada, Kai Liao, and Zong-Hong Zhu, Astrophys. J. 874, 139 (2019)
- Yufeng Li, Xilong Fan, and Lijun Gou, Astrophys. J. 837, 37 (2019)
- Kai Liao, Xuheng Ding, Marek Biesiada, Xi-Long Fan, and Zong-Hong Zhu, Astrophys. J. 867, 69 (2018)